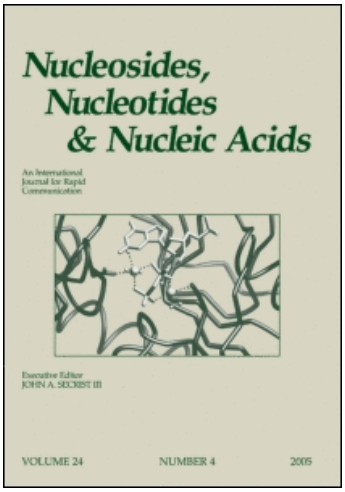

Nucleosides, Nucleotides and Nucleic Acids
Publication details, including instructions for authors and subscription information:
http://www.informaworld.com/smpp/title~content=t713597286

A Novel Stable RNA Pentaloop that Interacts Specifically with A Motif Peptide of Lambda-N Protein

Junji Kawakami[ab]; Naoki Sugimoto[ab]; Hisanori Tokitoh[b]; Yoshiatsu Tanabe[b]
[a] Frontier Institute for Biomolecular Engineering Research (FIBER), Konan University, Higashinada-ku, Kobe, Japan [b] Department of Chemistry, Faculty of Science and Technology, Konan University, Higashinada-ku, Kobe, Japan

To cite this Article Kawakami, Junji , Sugimoto, Naoki , Tokitoh, Hisanori and Tanabe, Yoshiatsu(2006) 'A Novel Stable RNA Pentaloop that Interacts Specifically with A Motif Peptide of Lambda-N Protein', Nucleosides, Nucleotides and Nucleic Acids, 25: 4, 397 — 416
To link to this Article: DOI: 10.1080/15257770600684027
URL: http://dx.doi.org/10.1080/15257770600684027

Nucleosides, Nucleotides, and Nucleic Acids, 25:397–416, 2006

ISSN: 1525-7770 print / 1532-2335 online
DOI: 10.1080/15257770600684027

Taylor & Francis
Taylor & Francis Group

A NOVEL STABLE RNA PENTALOOP THAT INTERACTS SPECIFICALLY WITH A MOTIF PEPTIDE OF LAMBDA-N PROTEIN

Junji Kawakami and Naoki Sugimoto □ *Frontier Institute for Biomolecular Engineering Research (FIBER), Konan University, Higashinada-ku, Kobe, Japan, and Department of Chemistry, Faculty of Science and Technology, Konan University, Higashinada-ku, Kobe, Japan*

Hisanori Tokitoh and Yoshiatsu Tanabe □ *Department of Chemistry, Faculty of Science and Technology, Konan University, Higashinada-ku, Kobe, Japan*

□ *To achieve a novel specific peptide–nucleic acid binding model, we designed an* in vitro *selection procedure to decrease the energetic contribution of the electrostatic interaction in the total binding energy and to increase the contribution of hydrogen bonding and π–π stacking. After the selection of hairpin-loop RNAs that specifically bound to a model peptide of lambda N protein (N peptide), a new thermostable pentaloop RNA motif (N binding thermostable RNA hairpin: NTS RNA) was revealed. The obtained NTS RNA was able to bind to the N peptide with superior specificity to the boxB RNA, which is the naturally occurring partner of the lambda N protein.*

Keywords Lambda N protein; Stable RNA hairpin; Specific binding; Thermodynamic analysis

INTRODUCTION

It is known that many biological events are evoked by the interaction between proteins and nucleic acids. The protein-nucleic acid interaction is a complex phenomenon that is achieved by many local interactions with various side residues of amino acids and nucleotides.[1–3] To resolve the complexity of the protein–nucleic acid interactions, specific model systems constructed with careful consideration about the contribution of each local interaction are particularly useful. The binding energy of a protein–nucleic acid interaction system is determined by electronic charge–charge

Received 26 December 2005; accepted 1 January 2006.

This work was supported in part by Grants-in-Aid for Scientific Research and the "Academic Frontier" Project (2004–2009) from the Ministry of Education, Culture, Sports, Science and Technology, Japan.

This article is dedicated to Professor Eiko Ohtsuka on the occasion of her 70th birthday.

Address correspondence to Junji Kawakami or Naoki Sugimoto, Frontier Institute of Biomolecular Engineering Research (FIBER), Konan University, 8-9-1 Okamoto, Higashinada-ku, Kobe 658-8501, Japan. E-mail: kawakami@konan-u.ac.jp, sugimoto@konan-u.ac.jp

interactions, hydrogen bonding networks, van der Waals interactions, and hydrophobic interactions as well as the participation of metal ions and water molecules. Among these, electrostatic interaction, a long-range interaction, increases the association rate of the protein–nucleic acid binding[4] and is certainly indispensable for a tight binding. However, nonspecific attractive force between positive charges on the amino acid side chains and negative charges on the nucleotide backbone is always accompanied by the electrostatic interaction between a basic protein and a nucleic acid. Sometimes this intrinsically nonspecific interaction is dominant even in a "sequence specific" binding. The hydrogen bonding network, on the other hand, is essential for the specific protein–nucleic acid interaction.[5,6] Also, London dispersion in π–π stacking is effective within an extremely short range, and therefore, the stacking is responsible for stabilization of macromolecular complexes with restricted structures in specific bindings.[7,8]

Here, we aimed to develop a model system of specific protein–nucleic acid interaction with desired binding mode. In the desired system, energetic contribution of the electrostatic interaction in the total binding energy of the model system should be small for the specificity, and instead, the contribution of hydrogen bonding and π–π stacking should be large. We paid notice to the interaction between lambda N protein and boxB RNA hairpin[9–15] as a mother system that contained all the electrostatic, hydrogen bonding, and π–π stacking interactions as described in detail in Results section. We designed a hairpin-loop RNA selection scheme with the model peptide of the N protein with 22 amino acids (N peptide) shown in Figure 1a as a target. In the selection scheme, negative selection step with highly positive charged peptide as a pseudotarget was placed before the positive selection step and

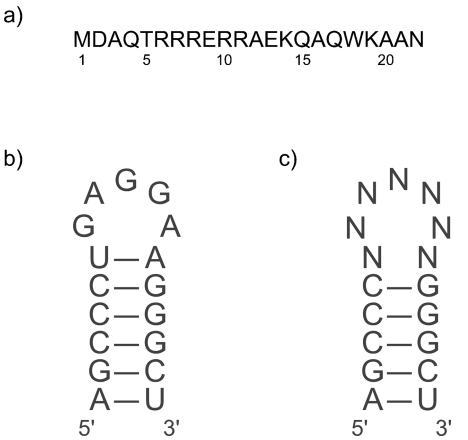

FIGURE 1 Sequences of N peptide, boxB RNA, and RNA library used in this study. (a) Sequence of the N peptide. (b) Sequence and proposed secondary structure of the boxB RNA. (c) Sequence and proposed secondary structure of the hairpin-loop RNA library with 7 nts randomized region. N denotes any nucleotide base (A, G, C, or U).

RNAs that bound to the pseudotarget molecule in nonspecific manner was removed from the RNA library. The winner RNA of our selection, to construct a model system in which π–π stacking and hydrogen bonding make large contribution to the binding and nonspecific electrostatic interaction does not, may not be the most forceful binder but should have sufficient specificity to its cognate target. As a result, a novel thermostable pentaloop RNA hairpin (N binding thermostable RNA hairpin: NTS RNA) was obtained. Based on thermodynamic data, it is expected that the NTS RNA binds to the N peptide with superior specificity to the boxB RNA, the naturally occurring partner of the lambda N protein.

MATERIALS AND METHODS

Preparation of Oligonucleotides and RNA Library

A template DNA with 40 nts for the polymerase chain reaction (PCR); 5′-GGCACATTCCAGCCCNNNNNNNGGGCTAACATTCAGATCC-3′, a 32 nts plus primer; 5′-AGTAATACGACTCACTATAGGCACATTCCAGC-3′, and a 16 nts minus primer; 5′-CGATTGTAAGTCTAGG-3′ were synthesized by the phosphoramidite method using a model 391 DNA/RNA synthesizer (PE Biosystems; PE). The NTS RNA, 5′-rAGCCCGGCUAACGGGCU-3′, and the boxB RNA, 5′-rAGCCCUGAAGAAGGGCA-3′, were similarly synthesized with additional treatment by 2 M tetrabutylammonium fluoride for 12 h to remove the 2′ *t*-butyldimethylsilyl group. After deblocking of the bases by overnight treatment with concentrated ammonia, the oligonucleotides were purified by high-performance liquid chromatography (HPLC) on a C-18 cartridge column TSK Gel (TOSOH). A double-stranded template DNA of transcription *in vitro* was prepared by PCR on a model 480 DNA thermal cycler (PE) with the single stranded template DNA and 100 pmol of each primer in 100 μL of reaction mixture containing 10 mM Tris HCl (pH 8.3), 50 mM KCl, 2.0 mM $MgCl_2$, 200 μM NTPs, and 2.5 U of AmpliTaq DNA polymerase (PE). Thirty cycles of PCR were carried out at 95°C for 60 s, 42°C for 60 s, and 72°C for 120 s. The resulting DNA product was recovered by ethanol preparation. A 40 nts RNA library that has the same sequence as the chemically synthesized template DNA except for U instead of T was then prepared using the AmpliScribe T7 transcription kit (Epicentre Technologies). The transcript RNA was purified from 8% denaturing polyacrylamide gel containing 8 M urea.

Preparation of Peptides

Peptides were synthesized with an Fmoc strategy on a solid support as described previously.[16] A solid support of Fmoc-NH-SAL resin (*N*-α-9-fulorenylmethoxy-carbonyl-super acid labile polystylene resin),

producing an amide at the carboxy terminus, was used in this study, and it was treated with piperidine to remove Fmoc group for the coupling. Protected Fmoc-amino acids (Watanabe Chemical) were activated their carboxyl group by three molar amounts of benzotriazolyl-*N*-oxytris(dimethylamino)phosphonium, 1-hydroxylbenzotriazole, and six molecular amounts of *N*,*N*-diisopropylethylamine, and coupled to the elongation peptide on the resin. After Fmoc deprotection of the last amino acid, amino terminus was biotinylated by Biotin-AC5 Sulfo-OSu (Dojindo) if needed. The synthesized peptides were cleaved from the resin and deprotected by trifluoroacetic acid with *m*-cresol, 1,2-ethanedithiol, and triethylsilyl bromide. These peptides were purified by the HPLC.

In vitro Selection

The transcribed RNA pool was quantified by measuring the absorbance at 260 nm with averaged extinction coefficients of the dinucleotides. Affinity columns were prepared by 0.5 nmol ImmunoPure Immobilized Avidin Gel (PIERCE) binding to biotinylated glycine (Gly), Tat peptide (RKKRRQRRR), or N peptide (MDAQTRRRERRAEKQAQWKAAN). Fifty picomoles of an RNA library in 200 μL of the binding buffer [10 mM Na_2HPO_4 (pH 7.0), 100 mM NaCl, and 1 mM Na_2EDTA] was heated at 94°C for 5 min and then slowly cooled to room temperature. The annealed RNA solution was mixed with Gly or Tat peptide immobilized agarose in pre-columns and incubated at 25°C for 1 h to eliminate the RNAs that are able to bind to the column support or Tat peptide. Then eluted RNAs from the pre-column were incubated with the N peptide immobilized agarose at 25°C for 1 h. During this incubation, the peptide and RNA concentrations were 50 μM and about 100 μM, respectively. Unbound RNAs on the affinity resin were washed out with 3 column volumes (200 μL $\times$ 3) of the binding buffer. RNAs bound to their target N peptide were collected by 1-h incubation with 200 μL of 500 μM N peptide solution put through the binding buffer in the column. The eluted RNAs were recovered by ethanol precipitation and converted to a library RNA with the next generation number by reverse transcription coupled PCR and subsequent transcription under the same conditions as described above.

Cloning and DNA Sequencing

After three rounds of selection and amplification, the double stranded PCR products were blunted by T4 DNA polymerase (TAKARA). The blunted DNAs were collected by ethanol precipitation and phosphorylated at their 5′ end by T4 polynucleotide kinase (TOYOBO). The Resulting DNAs were ligated into the *Hinc* II site of the plasmid pUC118 with T4 DNA ligase (TAKARA). *E. coli* MV1184 was transformed by the ligated plasmid DNAs

and cultured on an LB plate containing ampicillin, IPTG (isopropyl-β-*D*-thiogalactoside), and X-gal (5-bromo-4-chloro-3-indolyl-β-*D*-galactoside). After the blue-white selection, 20 white colonies were picked up and cultured in the LB medium containing ampicillin. The plasmids were recovered from *E. coli* clones using the alkaline lysis procedure. Nucleotide sequences were determined by the ABI PRISM 310 Genetic Analyzer (PE) using the BigDye termination method.

UV Measurements

An absorbance vs. temperature curve was determined at 260 nm with a Hitachi U-3210 spectrophotometer connected to a Hitachi SPR-10 thermoprogrammer in a 0.1 cm path length cuvette. The heating rate was 0.5 or 1°C/min. The water condensation on the cuvette exterior in the low temperature range was avoided by flushing with a constant stream of dry N_2 gas. All experiments were carried out in a buffer containing 10 mM Na_2HPO_4, 0.1 mM Na_2EDTA, pH 7.0. The extinction coefficients at 260 nm were calculated with the nearest-neighbor approximation.[17] The resulting values are 1.70×10^5 $cm^{-1}\,M^{-1}$ and 1.60×10^5 $cm^{-1}\,M^{-1}$ for the boxB RNA and the NTS RNA, respectively. The concentrations of the RNAs were determined from the absorbance measured at a high temperature.

Fluorescence Measurements

The fluorescence spectra of the peptide–RNA complexes were measured by a fluorescence F-3010 spectrophotometer (Hitachi) at a controlled temperature (25.0°C) by a thermostatic circulator. The peptide concentration was determined from the UV absorption of the Trp residue at 278 nm. All measurements were done in 10 mM phosphate buffer (pH 7.0) containing 100 mM NaCl and 0.1 mM Na_2EDTA. Fluorescence spectra were obtained every 1 nm at a scan rate of 50 nm min^{-1}. Fluorescence quenching of the peptides with the addition of the oligonucleotides was measured by the fluorescence intensity change at 350 nm with an excitation wavelength at 278 nm. The peptide concentration was 5 μM for all the fluorescence measurements.

The binding constant (K_a) of peptide-RNA complexes was estimated by the curve fitting procedure using the following equation:[16]

$$\Delta F = \Delta F_{\max}\Big\{K_a \cdot ([\text{RNA}] + [\text{Peptide}]) + 1 - \Big\{(K_a \cdot [\text{RNA}] + K_a \cdot [\text{RNA}] + K_a \cdot [\text{Peptide}] + 1)^2 - 4 \cdot K_a^2 \cdot [\text{Peptide}] \cdot [\text{RNA}]\Big\}^{1/2} \Big/ (2 \cdot K_a \cdot [\text{Peptide}])\Big\}$$

where ΔF is an observed fluorescence change and $\Delta F_{\max}$ is a maximum fluorescence change. The [Peptide] and [RNA] are the total peptide and added RNA concentrations, respectively. One RNA binding to one peptide

molecule in a non-cooperative manner was assumed for the correction of the RNA concentration term. The titration curves were analyzed by the nonlinear least-squares fitting procedure. Free energy changes at 25°C (ΔG°_{25}) were calculated from the rate constants as follows: $\Delta G^{\circ}_{25} = -298.15 R \ln K_a$, where R is the gas constant.

Surface Plasmon Resonance (SPR) Measurements

The peptide–RNA interaction was also examined using an SPR system with BIAcore 1000 (Pharmacia) by measuring the function of the mass change on the matrix surface. For the peptide immobilization on the SPR sensor chip, biotinylated peptide solution was injected onto streptavidin attached carboxymethylated dextran matrix on the gold sensor surface. RNA binding to the immobilized peptides was monitored by passing the RNA solution (5.0μM) in 10 mM phosphate buffer containing 100 mM NaCl and 0.1 mM Na_2EDTA (pH 7.0) across the sensor chip at a constant flow rate of 15 μL min^{-1} at 25°C. The SPR signals were collected every 1.0 s. The RNA solution was injected for 100 s and then the analyte solution was exchanged to the buffer without RNA. RNAs bound to the immobilized peptides were turned off by a flash flow of 0.05% SDS (sodium dodecyl sulfate) solution to regenerate the surface.

RESULTS

System Design for the Selection

For DNA, the double-stranded helix is the ordinary structure. Therefore, almost all the DNA binding proteins recognize the groove of the double stranded DNA whether the interaction is specific or not.[1,18–20] In contrast, higher ordered structures of RNA are defined by intramolecular interactions and are varied with many single stranded regions, i.e., bulges, internal loops, and hairpin-loops in addition to the double stranded regions. These particular local structures of RNA frequently participate in the specific interaction with proteins.[15,21–24] We have already observed the importance of the specific structure of RNA for a peptide–nucleic acid binding system in our previous study to obtain peptides that recognize stable tetraloop structures of nucleic acids *via* combinatorial chemistry.[25] At that time, in our tiny model systems, π–π stacking of an aromatic side residue and nucleotide base played a significant role for the binding. When a flipped nucleobase in the loop was exposed to the solvent water, many aromatic amino acids were selected whereas a dominant force was brought by hydrogen bonds. From this information, here, π–π stacking in addition to hydrogen bonding was settled as an important interaction for obtaining specific model system. For π–π stacking, a nucleic acid structure should be enough stable and restricted

to expose an aromatic base portion at a specific position in the structure. Fortunately, we were able to use the DNA counterpart of the stable rC(UUCG)G hairpin[26–30] in our previous study.[25] However, there are only a few examples that are admirably adapted for use as a model system in nature, and consequently, in this study we decided to select such a nucleic acid structure from a random library.

Regarding the protein part, some RNA binding motifs as functional partial structures of the RNA binding proteins are the candidates for use. However, the ribonucleoprotein (RNP) consensus sequence[31,32] and RNP K homology motif[33,34] in RNPs such as U1A are rather large, i.e., 50 to 100 amino acids, and thus are not suitable for the tiny model construction. Although the RGG box containing arginine–glycine–glycine tripeptide repeat is as small as 20 to 25 amino acids,[35] this is an intrinsically nonspecific binding motif and is also not appropriate for the model system. On the other hand, the highly basic arginine rich motif seen in some proteins such as the Tat or Rev protein of the human immunodeficiency virus is able to achieve sequence specific RNA binding using only 10 to 20 amino acids.[19,21,22,36,37] Therefore, this tiny motif is the most adequate for the model system, although π–π stacking is not fundamentally contained in the interaction between the arginine rich motif and RNA. Among the proteins with the arginine rich motif, the lambda N protein interacts with its cognate RNA hairpin-loop structure by using π–π stacking.

The lambda N protein regulates the anti-termination of transcription by way of the binding to a boxB hairpin-loop in the transcript mRNA.[9–15,38,39] In the stable N protein–boxB hairpin-loop complex, many interactions are concerned with the binding: electrostatic interaction between basic amino acids and phosphate backbone, hydrophobic interaction between alanine 3 and the stem region of the hairpin-loop structure, the hydrogen bond network, and π–π stacking of the aromatic side residues between tryptophan 18 and adenosine 9.[40] Furthermore, a model peptide of the N protein (N peptide) shown in Figure 1a is able to bind to a model RNA of the boxB hairpin-loop (boxB RNA) shown in Figure 1b with the same sequence specificity and binding stability as the natural N-boxB interaction.[10–12]

From the knowledge mentioned above, we have selected hairpin-loop RNAs that bind to the N peptide from a hairpin-loop RNA library with a 7 nucleotides (nts) random region as shown in Figure 1c. Because it is thought that the energetic contribution of π–π stacking is rather weak even in a sequence specific protein–nucleic acid interaction,[7,41,42] the best way for increment the energetic contribution of hydrogen bonding and π–π stacking in the total binding energy is decrement the electrostatic contribution in the binding. In the selection scheme, negative selection step with highly positive charged peptide as a pseudotarget was placed before the positive selection step and RNAs that bound to the pseudotarget molecule in

nonspecific manner by using electrostatic interaction mainly was removed from the RNA library.

Selection of N Peptide–Binding RNAs

The N peptide–binding RNAs were selected from a library shown in Figure 1c containing about 1.7×10^4 random sequences with 3, 5, or 7 nts loops. Using the procedure shown in Figure 2, the RNAs that bound to column resin were removed from the library by passing them through a column with glycine immobilized resin (Gly column). Individually, the RNAs that interact nonspecifically with a basic peptide by an electrostatic effect were eliminated from the other library by passing them through a column with the resin on which a model peptide (RKKRRQRRR) of the highly basic Tat protein was immobilized (Tat column). RNAs after those pretreatments were incubated in a column with the N peptide immobilized resin (N column) separately and the N binding RNAs were recovered by an affinity elution procedure with the binding buffer containing 0.5 mM N peptide.

The peptide binding property of RNAs in the initial library before the selection (Generation 0; G0) and in the libraries after three cycles of the selection (Gly-G3 and Tat-G3) were examined. The library RNA was passed through the affinity columns and the amount of retained RNA in the columns

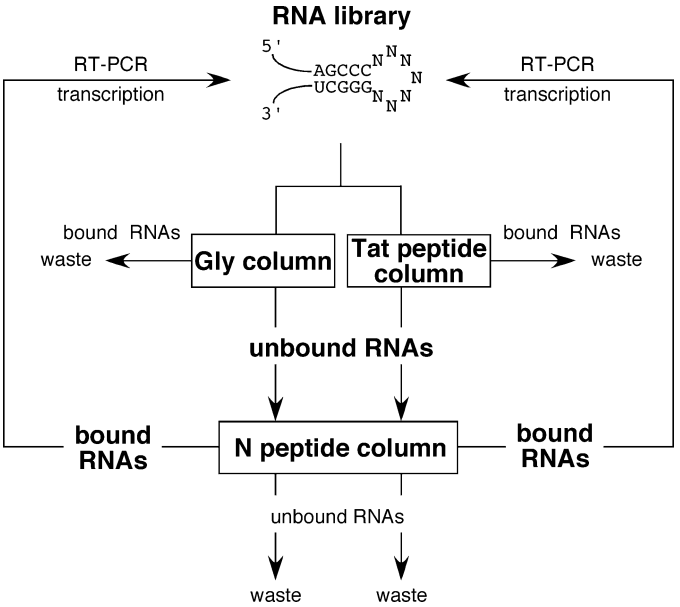

FIGURE 2 Selection procedure with affinity columns used in this study. An RNA library was passed through columns in which Tat peptide or Gly was immobilized. Then the eluted RNAs were loaded to the N peptide column. RNAs were incubated in each column for 1 h at 25°C in a buffer containing 10 mM Na_2HPO_4 (pH 7.0), 100 mM NaCl, and 1 mM Na_2EDTA. After washing with three column volumes of the buffer, bound RNAs were eluted from the column by a buffer containing 0.5 mM N peptide.

was determined separately. As shown in Figure 3a and Table 1, the N peptide binding RNAs were concentrated during both selections; 47.0 and 45.3% of the total amount of RNAs in the Gly-G3 and Tat-G3 libraries were bound to the N column, respectively, whereas only 27.3% of the RNAs in the G0 library bound to the N column. On the other hand, the amount of Tat peptide binding RNAs (nonspecific binders) decreased in the Tat-G3 library from 46.0 (G0) to 38.0%. In contrast, the amount of the nonspecific binders

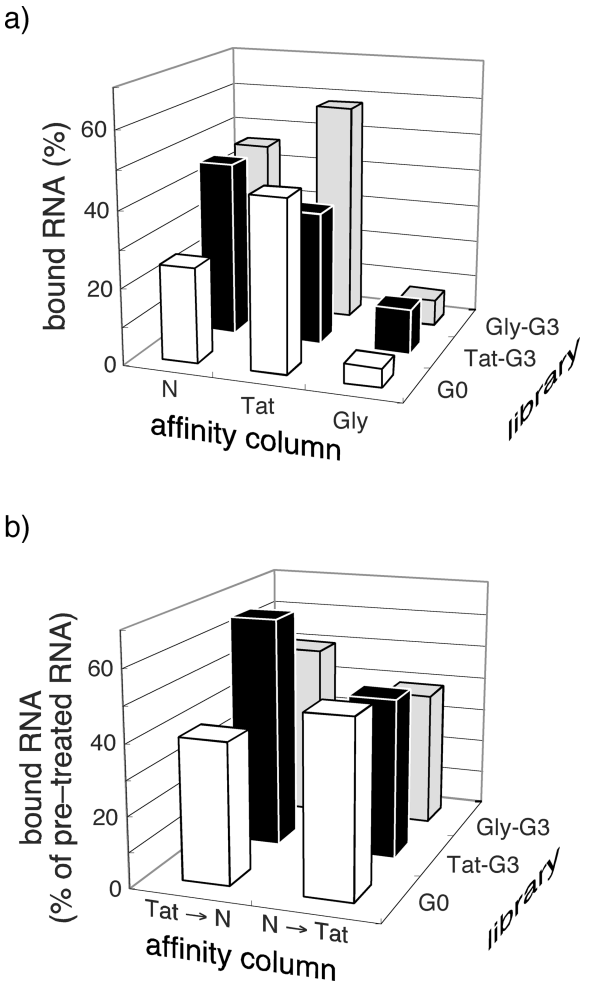

FIGURE 3 Binding properties of hairpin-loop RNA libraries to Tat, N, and Gly columns. (a) Percentages of the bound RNA in the total amount of RNA in the libraries to the columns. Amount of the bound RNA was calculated from UV absorption of eluted RNA at 260 nm. The white, black, and gray bars indicate the G0, Tat-G3, and Gly-G3 libraries, respectively. (b) Percentages of the bound RNA to the columns for the libraries after negative selection procedures. Tat → N indicates the amount of N peptide binding RNA in the library RNA that eluted from (did not bind to) the Tat column. This is the mimetic condition of the selection procedure for the Tat-G3 library. N → Tat indicates the amount of Tat peptide binding RNA in the library after the negative selection with the N column, similarly.

TABLE 1 Percentages of Bound RNA to Affinity Columus[a]

Library	Affinity column				
	N	Tat	Gly	Tat → N	N → Tat
Gly-G3	47.0 ± 1.7	57.3 ± 2.1	9.3 ± 2.5	51.0 ± 3.6	40.0 ± 2.6
Tat-G3	45.3 ± 4.0	38.0 ± 3.0	11.7 ± 2.5	70.3 ± 4.0	48.3 ± 2.5
G0	27.3 ± 2.1	46.0 ± 1.7	8.3 ± 2.9	40.3 ± 2.5	50.7 ± 2.1

[a]RNA libraries were incubated in each colmun for 1 h at 25°C and then washed with three columun volumes of the binding buffer. Percentages of the bound RNAs to columns were calculated from UV absorption of eluted RNAs at 260 nm. See the legend of Figure 3 for the abbreviations Tat → N and N → Tat.

increased in the Gly-G3 library from 46.0 to 57.3%. In other words, it was proved that specific binders to the N peptide were selectively concentrated in the Tat-G3 library. Similar results were obtained from the experiments that mimicked the selection procedures as shown in Figure 3b and Table 1. After the negative selection procedure, more than 70% of RNAs in the Tat-G3 library bound to the N column (Tat → N), indicating the specific binding of RNAs in the Tat-G3 library to the N peptide. No such concentration of specific binder could be seen for Gly-G3 library after the negative selection.

Nucleotide Sequences of N Peptide Binding RNAs

Figure 4 shows the nucleotide sequences of 20 clones from the Gly-G3 and Tat-G3 library. As a result, almost all the clones from the Gly-G3 library had 7 nts loop and no consensus sequence was found in the nucleotide sequences. On the other hand, an obvious consensus sequence was revealed from the Tat-G3 library as shown in Figure 4. The consensus sequence was 5′-GGYYRRC-3′, where Y and R indicate the pyrimidine (U or C) and purine nucleotides (A or G), respectively, and the most abundant sequence was 5′-GGCUAAC-3′. This consensus sequence suggests that the clones in the Tat-G3 library have a 5 nts loop (pentaloop) closed by a GC base pair. The consensus sequence in the Tat-G3 library was different from the natural lambda boxB RNA sequence, 5′-UGAARAA-3′. For example, closing the base pair of the loop was GC in the consensus sequence whereas it was U/A in the natural boxB RNA. The bases in the loop also differ except for the first G and the fourth purine nucleotide.

Structural Stability of N Peptide Binding RNAs

UV melting behaviors of the boxB RNA (5′-rAGCCCUGAAGAAGGGCA-3′) and a model RNA from the consensus sequence of the Tat-G3 clones, (5′-rAGCCCGGCUAACGGGCA-3′: NTS RNA) are shown in Figure 5 (nucleotides in the loop region are underlined). As seen in Figure 5, both RNAs melt in the higher temperature region above 80°C, although a small

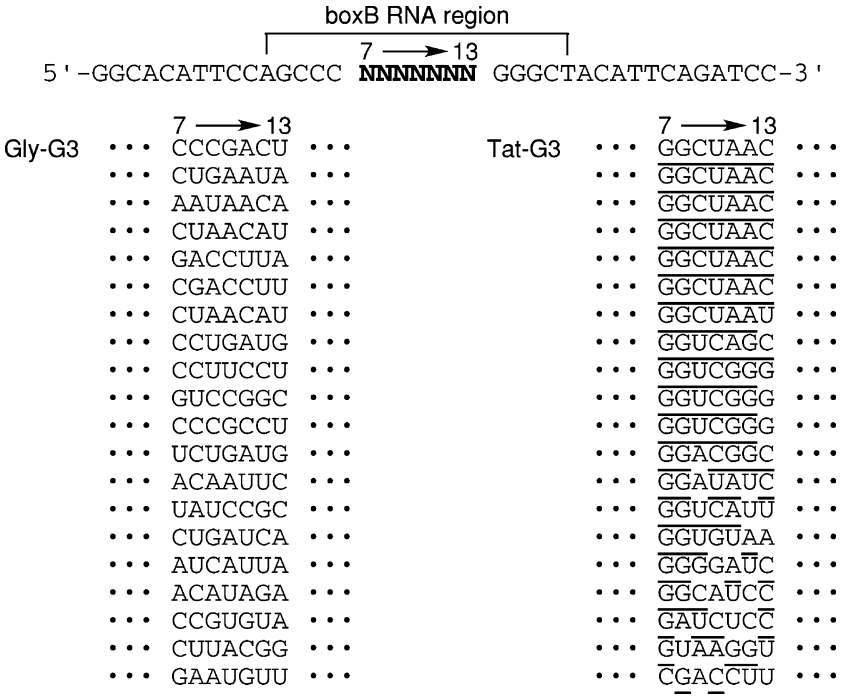

FIGURE 4 Nucleotide sequences of N peptide binding RNAs. RNAs after three cycles of the selection were inserted into pUC118 plasmid and cloned. These sequences were obtained from independent 20 clones of each library (Gly-G3 and Tat-G3). The nucleotides correspond to the consensus GGYYRRC (Y = C/U, and R = A/G) were underlined for the Tat-G3 clones.

transition of the baseline was observed within the temperature range from 30 to 50°C for the NTS RNA. UV melting behaviors of the RNAs at 5 μM and 50 μM did not change for both RNAs. The stability of the NTS RNA structure was also evaluated using native polyacrylamide gel electrophoresis (data not shown). The mobility of the NTS RNA at 20°C resembled that of hairpin-loop DNAs with 17 or 18 nts but was different from the mobility of a 17 base-paired-double-stranded DNA. Same tendency could be seen in the PAGE experiment at 50°C. The results from the gel electrophoresis indicated that the NTS RNA folds into almost the same hairpin-loop structure at both temperatures of 20 and 50°C.

Binding Property of the N Peptide–Binding RNAs to the N Peptide

Binding affinity of the RNAs to the N peptide was analyzed using SPR. As the result, about 80 and 70 response unit (RU) increments were observed by 100 sec passing 5.0 μM of the RNAs across the N peptide immobilized sensor surface for the boxB RNA and the NTS RNA, respectively (data not shown). This result suggests the slightly weaker binding ability of the NTS RNA to the N peptide than that of the boxB RNA. However, for the experiments

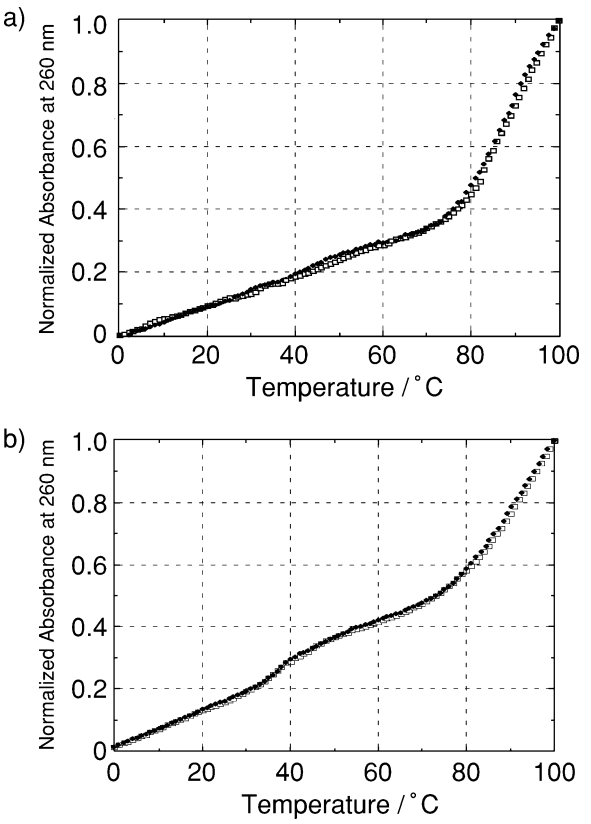

FIGURE 5 Normalized absorbance vs temperature curves for (a) 5′-rAGCCCUGAAGAAGGGCU-3′ (boxB RNA) and (b) 5′-rAGCCCGGCUAACGGGCU-3′ (NTS RNA). Nucleotides in the loop region were underlined. All mesurements were done in a buffer containing 10 mM Na_2HPO_4 (pH 7.0), 100 mM NaCl, and 1 mM Na_2EDTA. The oligonucleotide concentrations were 5 μM (open diamond) and 50 μM (closed diamond).

with the Tat peptide immobilized sensorchip, the RU increment was about 60 and 30 for the boxB RNA and the NTS RNA, respectively. In other words, the NTS RNA discriminated the two highly basic peptides, whereas the boxB RNA interacted with both peptides. The response of the NTS RNA binding to the N peptide changed more slowly than that in the other cases.

Quantification of Interaction between the N Peptide and N Peptide–Binding RNAs by Fluorescent Quenching

The binding constants of the RNAs and N peptide were also analyzed *via* the fluorescence of tryptophan. As shown in Figure 6, the fluorescent quenching of tryptophan[44] in the N peptide was observed by titration of the NTS RNA. The quenching behavior exhibited exponential dependency to the concentration of the NTS RNA. Therefore, those results strongly suggest that the NTS RNA utilize the π–π stacking for the binding to the

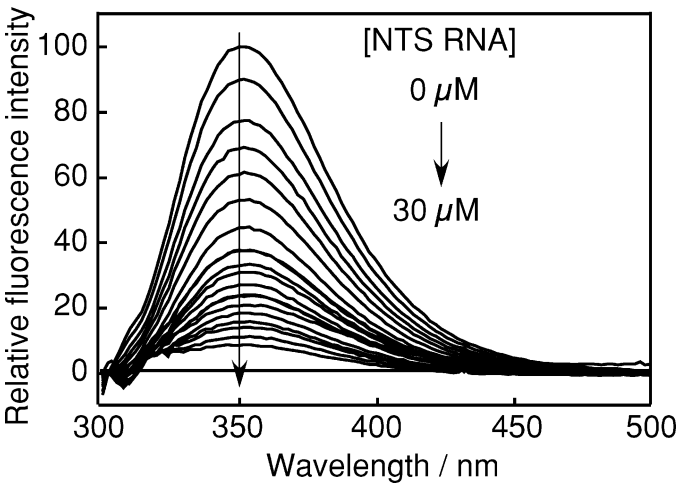

FIGURE 6 Fluorescence quenching of tryptophan in the N peptide accompanied by NTS RNA titration. Concentration of the N peptide was 5 μM. All measurements were done with an excitation wavelength at 278 nm in a buffer containing 10 mM Na_2HPO_4 (pH 7.0), 100 mM NaCl, and 1 mM Na_2EDTA at 25°C.

N peptide just like as boxB RNA. Maximum quenching fractions of the fluorescence were almost the same value; 86.4 and 85.7% for the boxB RNA and the NTS RNA, respectively. The binding constant, K_a, of the N peptide binding was 1.37×10^8 M^{-1} and 3.36×10^7 M^{-1} at 25°C for the boxB RNA and the NTS RNA, respectively. These binding constants are equivalent to -11.1 and -10.3 kcal mol^{-1} as the free energy changes during the binding at 25°C (ΔG°_{25}). The difference in the binding affinity of the two RNAs was 0.8 kcal mol^{-1}.

DISCUSSION

In vitro Selection Procedure to Obtain N Peptide–Binding RNAs

Several selection of mutant N protein/peptide that interact with the boxB RNA were reported previously, indicating availability of another artificial combination.[43–47] For the RNA part, although point mutants were analyzed for the boxB RNA so far,[37,38,47,48] the tightest binder to the N peptide should be obtained from a library *via* normal *in vitro* selection experiments.[49] However, a novel selection procedure, in which a negative selection to remove the nonspecific tight binder to the target is included, would be required for obtaining an aimed RNA molecule that is a specific tight binder to the target with the desired binding mode. In this study, a model peptide of the Tat protein of the human immunodeficiency virus type-1 (Tat peptide) was used as the pseudotarget for the negative selection.[19,21] The Tat peptide is one of the best pseudotarget molecules that decreases the nonspecific electrostatic background but retains the π–π stacking, because the Tat peptide

contains many basic amino acids but does not have an aromatic residue. Independently, another selection procedure with Gly resin as a pseudotarget to remove the RNAs that are nonspecifically bound to the column support was simultaneously carried out. It is expected that the N peptide–binding RNAs with a large electrostatic background should be obtained from the library after the selection with pretreatment by the Gly resin.

From the analysis of the libraries after the selection procedures, the amount of the N peptide binding RNAs increased about 20% during both selections and the order of the amount of the N peptide–binding RNAs was G0 $\ll$ Gly-G3, Tat-G3 as shown in Figure 3a and Table 1. On the other hand, the order of the amount of the Tat peptide binding RNAs was Tat-G3 $<$ G0 $<$ Gly-G3. In other words, the Tat-G3 library contained abundant specific N peptide–binding RNAs as expected. Analogous results were appeared in the experiments to elucidate the effect of the pretreatments as shown in Figure 3b and Table 1. About 40–50% of the RNAs that did not bind to the N column (after the pretreatment with N column) were bound to the Tat column for all the libraries (N $\rightarrow$ Tat). This result corresponds to the finding that 46% of the RNAs in the G0 library (before selection) is bound to the Tat column, indicating 40–50% of the random RNAs have potential ability of binding to the Tat peptide. Contrary to the results of N $\rightarrow$ Tat, the amount of the N peptide binding RNAs in G0, Gly-G3, and the Tat-G3 libraries after the negative selection procedure with the Tat column was about 40, 50, and 70%, respectively (Tat $\rightarrow$ N). These results suggest the following two things: (a) Many N peptide binding RNAs in the Gly-G3 library interact with the N peptide *via* an electrostatic interaction and thus they also bind to the Tat peptide, and (b) N peptide binding RNAs in the Tat-G3 library interact with the N peptide by using π–π stacking and hydrogen bonding with reduced energetic contribution of electrostatic interaction and thus their affinity to the Tat peptide is low. In this manner, the specific N peptide binding RNAs were concentrated in the Tat-G3 library as we desired.

Nucleotide Sequences of N Peptide–Binding RNAs

The nucleotide sequences of 20 clones from the Gly-G3 and Tat-G3 libraries were compared with that of the natural boxB hairpin-loop RNA. As shown in Figure 4, almost all the clones from the Gly-G3 library had a 7 nts loop but a consensus sequence could not be found. This result suggests that the RNAs in the Gly-G3 library expose their phosphate group to the solvent water to stabilize the N peptide–RNA binding by electrostatic interaction, and therefore, any restricted structure with an ordered orientation of the bases would not exist. Thus, the interaction between the RNAs in the Gly-G3 library and the N peptide should be nonspecific. This conclusion is similar to the entire character of the Gly-G3 library mentioned above and consistent with the adsorption result on the affinity columns.

On the other hand, the nucleotide sequence of the clones in the Tat-G3 resembled each other and a consensus sequence with a pentaloop, 5′-GGYYRRC-3′, was revealed. This consensus sequence was distinct from the natural boxB RNA sequence, 5′-UGAARAA-3′. Mutation analysis showed the sequence could be changed in some extent; however, the valid sequence 5′-UGRRRAA-3′ was not consistent with our result either.[37,38] The closing base pair of the loop was G/C in our consensus sequence, whereas it was U/A in the natural boxB hairpin-loop RNA. Only a transversion of the closing base pair from U/A to A/U leads to a drastic decrease in the binding constant of the N peptide–boxB RNA complex.[37] Also, similar results were reported for the natural N protein–boxB hairpin-loop binding both *in vitro* and *in vivo*.[37,39] Consequently, the consensus sequence obtained from the Tat-G3 library should fold into a novel structure that is different from the structure of the natural boxB. The natural boxB RNA has many purine bases in the loop and folds into a highly ordered structure that resembles the GNRA tetraloop.[12] Our consensus sequence from the Tat-G3 library has two pyrimidine bases at the second and third positions of the loop so that the consensus sequence may fold into a ordered structure that resembles UNCG rather than GNRA and exposes a pyrimidine base to the solvent for π–π stacking.[50,51] The phosphate groups in the folding of the consensus sequence might be buried within the packed structure.

Structural Stability of N Peptide–Binding RNAs

The UV melting behavior showed the structural transition of the boxB RNA and the NTS RNA in the higher temperature region above 80°C. Because a nucleic acid with a hairpin-loop structure has complementary sequences at both its ends, it may interact with another molecule to form a duplex with an internal loop. Therefore, it is necessary to confirm the original structure corresponding to the melting behavior. For the self-complementary duplex, the melting behavior depends on the nucleic acid concentration and the melting temperature, T_m, could be defined as $T_m^{-1} = (2.303R \log C_t + \Delta S^\circ)/\Delta H^\circ$; where R, C_t, ΔS°, and ΔH° are the gas constant, the total strand concentration of the nucleic acid, and the entropic and enthalpic changes for the duplex formation, respectively. When the nucleic acid folds into a hairpin-loop structure itself, the melting temperature is independent of the strand concentration. The UV melting experiments for two RNA samples with different concentrations were carried out and the results were compared as shown in Figure 5. As a result, the UV melting behaviors of the RNAs at 5 μM and 50 μM did not change for both RNAs, and therefore, the NTS RNA should fold into a hairpin-loop structure as well as the boxB RNA. The high melting temperature above 80°C denotes an extraordinarily stable hairpin-loop structure of the NTS RNA like the GNRA tetraloop with a melting temperature above 70°C.[53]

A small transition in the baseline was observed within the temperature range from 30 to 50°C for the NTS RNA, so that the possibility of a drastic conformational change in the temperature range was confirmed by the PAGE experiments (data not shown). As a result, the mobility of the NTS RNA resembled that of the 17 or 18 nts hairpin-loop DNAs with a stable GNRA tetraloop but was different from the mobility of a 17 base-paired-double-stranded DNA at both temperatures of 20 and 50°C. These results indicated that the NTS RNA folds into the hairpin-loop structure at both temperatures of 20 and 50°C and that the drastic conformational change will not be observed within the temperature range. This small transition at the lower temperature range was not affected by the nucleic acid concentration and thus this transition might be due to some local structural change in the loop region.

Affinity and Specificity of N Peptide Binding RNAs

The affinity of the N peptide binding RNAs to the N peptide was evaluated by the fluorescent quenching of tryptophan. As a small structural transition of the NTS RNA from 30 to 50°C was suggested, all experiments were carried out at 25°C, which was the same temperature during the selection. There should be at least two binding modes when a positive charged peptide binds to a negative charged nucleic acid. One of the binding modes should correspond to the binding seen in the fluorescent quenching with π–π stacking to tryptophan and the other one should not be accompanied by the fluorescent quenching of tryptophan. Of course, the former is the specific binding with the desired interaction and the latter would be the nonspecific binding mainly due to the electrostatic interaction. The ΔG°_{25} values from the fluorescent quenching for the boxB RNA and the NTS RNA binding were -11.1 kcal mol^{-1} and -10.3 kcal mol^{-1}, respectively. The binding energy determined in this study was slightly smaller than that expected from the previous reports using the gel shift experiment[15,38] ($\Delta G^{\circ}_{25} = -11$ to -11.5 kcal mol^{-1}). The experimental condition, especially salt concentration, may cause the differences.

From the SPR analysis, it was found that the boxB RNA bound rapidly to both peptides, N and Tat. Also the NTS RNA bound to the Tat peptide rapidly. Only when the NTS RNA interacted with the N peptide, the response changed more slowly than the other cases at both the association and the dissociation phases (data not shown). Because a large electrostatic contribution during a binding event leads a large rate constant,[4] the energetic contribution of the electrostatic interaction in the NTS RNA–N peptide pair should be smaller than that in the other cases as expected. Furthermore, the difference of the response unit change ($\Delta\Delta R$) between the response by N peptide binding and that by Tat peptide binding at the end of the association phase in the NTS RNA case ($\Delta\Delta R = 40$) is larger than that in the case of boxB RNA ($\Delta\Delta R = 20$). This finding suggests that the NTS RNA

discriminated two highly basic peptides because the amount of the bound RNA to the peptides on the surface after infinite time relates to the binding constant. This consideration about the binding specificity agrees with the following facts. Binding property of the Tat-G3 library shown in Figure 3 suggests that the binding constant of the NTS RNA, the representative of the library, to the N peptide is almost 10 times larger than that to the Tat peptide. On the other hand, the boxB RNA and its analogous sequences were eliminated during the selection. This result suggests that the energetic difference of the boxB RNA binding to the Tat peptide and the N peptide is smaller than that of NTS RNA.

In summary, we realized to construct a novel tiny peptide–RNA interaction model by a selection procedure designed to increase the specificity of the model system. Although the affinity of the NTS RNA to the cognate target N peptide is 0.8 kcal mol^{-1} weaker than that of the boxB RNA, the specificity of the NTS RNA binding to the N peptide seems to exceed that of the boxB RNA due to repression of nonspecific force to the non-cognate target molecules. The NTS RNA folds into a highly thermostable hairpin-loop structure and specifically interacts with the N peptide by using its restricted structure. This stable hairpin-loop structure of the NTS RNA itself and applications of the NTS RNA *in vivo* and *in vitro* are of interest. It is of utmost importance that the N peptide–NTS RNA and their point mutants would be a useful model system for better understanding of many biological systems.

REFERENCES

1. Segal, D.J.; Barbas III, C.F. Design of novel sequence-specific DNA-binding proteins. Current Opinion in Chemical Biology **2000**, 4, 34–39.
2. Cheng, A.C.; Calabro, V.; Frankel, A.D. Design of RNA-binding proteins and ligands. Current Opinion in Structural Biology **2001**, 11, 478–484.
3. Barrick, J.E.; Roberts, R.W. Sequence analysis of an artificial family of RNA-binding peptides. Protein Science **2002**, 11, 2688–2696.
4. Selzer, T.; Albeck, S.; Schreiber, G. Rational design of faster associating and tighter binding protein complexes. Nature Structural Biology **2000**, 7, 537–541.
5. Cheng, A.C.; Chen, W.W.; Fuhrmann, C.N.; Frankel, A.D. Recognition of nucleic acid bases and base-pairs by hydrogen bonding to amino acid side-chains. Journal of Molecular Biology **2003**, 327, 781–796.
6. Cheng, A.C.; Frankel, A.D. Ab initio interaction energies of hydrogen-bonded amino acid side chain–nucleic acid base interactions. Journal of the American Chemical Society **2004**, 126, 434–435.
7. Nolan, S.J.; Shiels, J.C.; Tuite, J.B.; Cecere, K.L.; Baranger, A.M. Recognition of an essential adenine at a protein–RNA interface: Comparison of the contributions of hydrogen bonds and a stacking interaction. Journal of the American Chemical Society **1999**, 121, 8951–8952.
8. Luchansky, S.J.; Nolan, S.J.; Baranger, A.M. Contribution of RNA conformation to the stability of a high-affinity RNA–protein complex. Journal of the American Chemical Society **2000**, 122, 7130–7131.
9. Doelling, J.H.; Franklin, N.C. Effects of all single base substitutions in the loop of boxB on antitermination of transcription by bacteriophage lambda's N protein. Nucleic Acids Research **1989**, 17, 5565–5577.

10. Su, L.; Radek, J.T.; Hallenga, K.; Hermanto, P.; Chan, G.; Labeots, L.A.; Weiss, M.A. RNA recognition by a bent alpha-helix regulates transcriptional antitermination in phage lambda. Biochemistry **1997**, 36, 12722–12732.
11. Weiss, M.A.; Narayana, N. RNA recognition by arginine-rich peptide motifs. Biopolymers **1998**, 48, 167–180.
12. Legault, P.; Li, J.; Mogridge, J.; Kay, L.E.; Greenblatt, J. NMR structure of the bacteriophage lambda N peptide/boxB RNA complex: recognition of a GNRA fold by an arginine-rich motif. Cell **1998**, 93, 289–299.
13. Barrick, J.E.; Roberts, R.W. Achieving specificity in selected and wild-type N peptide–RNA complexes: The importance of discrimination against noncognate RNA targets. Biochemistry **2003**, 42, 12998–13007.
14. Austin, R.J.; Xia, T.; Ren, J.; Takahashi, T.T.; Roberts, R.W. Differential modes of recognition in N peptide–boxB complexes. Biochemistry **2003**, 42, 14957–14967.
15. Cilley, C.D.; Williamson, J.R. Structural mimicry in the phage phi21 N peptide–boxB RNA complex. RNA **2003**, 9, 663–676.
16. Nakano, S.; Sugimoto, N. Single-stranded DNA recognition of a 24-mer peptide derived from RecA protein. Bulletin of the Chemical Society of Japan **1998**, 71, 2205–2210.
17. Richards, E.G. Use of tables in calculation of absorption, optical rotatory dispersion, and circular dicroism of polyribonucleotides. In *Handbook of Biochemistry and Molecular Biology, 3rd ed., Nucleic Acids Vol. I.* CRC Press, Cleveland, Ohio **1975**, 596–603.
18. Juo, Z.S.; Chiu, T.K.; Leiberman, P.M.; Baikalov, I.; Berk, A.J.; Dickerson, R.E. How proteins recognize the TATA box. Journal of Molecular Biology **1996**, 261, 239–254.
19. Chen, L.; Frankel, A.D. A peptide interaction in the major groove of RNA resembles protein interactions in the minor groove of DNA. Proceedings of the National Academy of Sciences USA **1995**, 92, 5077–5081.
20. Negi, S.; Itazu, M.; Imanishi, M.; Nomura, A.; Sugiura, Y. Creation and characteristics of unnatural CysHis3-type zinc finger protein. Biochemical and Biophysical Research Communications **2004**, 325, 421–425.
21. Aboul-ela, F.; Karn, J.; Varani, G. The structure of the human immunodeficiency virus type-1 TAR RNA reveals principles of RNA recognition by Tat protein. Journal of Molecular Biology **1995**, 253, 313–332.
22. Battiste, J.L.; Mao, H.; Rao, N.S.; Tan, R.; Muhandiram, D.R.; Kay, L.E.; Frankel, A.D.; Williamson, J.R. α helix–RNA major groove recognition in an HIV-1 Rev peptide–RRE RNA complex. Science **1996**, 273, 1547–1551.
23. Cai, Z.; Gorin, A.; Frederick, R.; Ye, X.; Hu, W.; Majumdar, A.; Kettani, A.; Patel, D.J. Solution structure of P22 transcriptional antitermination N peptide–boxB RNA complex. Nature Structural Biology **1998**, 5, 203–212.
24. Das, C.; Frankel, A.D. Sequence and structure space of RNA-binding peptides. Biopolymers **2003**, 70, 80–85.
25. Kawakami, J.; Okabe, S.; Yoneyama, M.; Miyoshi, D.; Sugimoto, N. manuscript in preparation.
26. Kawakami, J.; Yoneyama, M.; Miyoshi, D.; Sugimoto, N. A stable DNA tetraloop and its structural tolerance for modification. Chemistry Letters **2001**, 258–259.
27. Heus, H.A.; Pardi, A. Structural features that give rise to the unusual stability of RNA hairpins containing GNRA loops. Science **1991**, 253, 191–194.
28. Antao, V.P.; Lai, S.Y.; Tinoco, I.Jr. A thermodynamic study of unusually stable RNA and DNA hairpins. Nucleic Acids Research **1991**, 19, 5901–5905.
29. Butcher, S.E.; Dieckmann, T.; Feigon, J. Solution structure of the conserved 16 S-like ribosomal RNA UGAA tetraloop. Journal of Molecular Biology **1997**, 268, 348–358.
30. Tuerk, C.; Gauss, P.; Thermes, C.; Groebe, D.R.; Gayle, M.; Guild, N.; Stormo, G.; d'Aubenton-Carafa, Y.; Uhlenbeck, O.C.; Tinoco, I.Jr.; Brody, E.N.; Gold, L. CUUCGG hairpins: extraordinarily stable RNA secondary structures associated with various biochemical processes. Proceedings of the National Academy of Sciences USA **1988**, 85, 1364–1368.
31. Oubridge, C.; Ito, N.; Evans, P.R.; Teo, C.H.; Nagai, K. Crystal structure at 1.92 A resolution of the RNA-binding domain of the U1A spliceosomal protein complexed with an RNA hairpin. Nature **1994**, 372, 432–438.
32. Allain, F.H.; Gubser, C.C.; Howe, P.W.; Nagai, K.; Neuhaus, D.; Varani, G. Specificity of ribonucleoprotein interaction determined by RNA folding during complex formulation. Nature **1996**, 380, 646–650.

33. Musco, G.; Stier, G.; Joseph, C.; Castiglione Morelli, M.A.; Nilges, M.; Gibson, T.J.; Pastore, A. Three-dimensional structure and stability of the KH domain: molecular insights into the fragile X syndrome. Cell **1996**, 85, 237–245.
34. Musco, G.; Kharrat, A.; Stier, G.; Fraternali, F.; Gibson, T.J.; Nilges, M.; Pastore, A. The solution structure of the first KH domain of FMR1, the protein responsible for the fragile X syndrome. Nature Structural Biology **1997**, 4, 712–716.
35. Burd, C.G.; Dreyfuss, G. Conserved structures and diversity of functions of RNA-binding proteins. Science **1994**, 265, 615–621.
36. Puglisi, J.D.; Chen, L.; Blanchard, S.; Frankel, A.D. Solution structure of a bovine immunodeficiency virus Tat-TAR peptide–RNA complex. Science **1995**, 270, 1200–1203.
37. Tan, R.; Frankel, A.D. Structural variety of arginine-rich RNA-binding peptides. Proceedings of the National Academy of Sciences USA **1995**, 92, 5282–5286.
38. Chattopadhyay, S.; Garcia-Mena, J.; DeVito, J.; Wolska, K.; Das, A. Bipartite function of a small RNA hairpin in transcription antitermination in bacteriophage lambda. Proceedings of the National Academy of Sciences USA **1995**, 92, 4061–4065.
39. Chattopadhyay, S.; Hung, S.C.; Stuart, A.C.; Palmer AG, 3.; Garcia-Mena, J.; Das, A.; Gottesman, M.E. Interaction between the phage HK022 Nun protein and the nut RNA of phage lambda. Proceedings of the National Academy of Sciences USA **1995**, 92, 12131–12135.
40. Weiss, M.A. RNA-mediated signaling in transcription. Nature Structural Biology **1998**, 5, 329–333.
41. LeCuyer, K.A.; Behlen, L.S.; Uhlenbeck, O.C. Mutagenesis of a stacking contact in the MS2 coat protein–RNA complex. EMBO Journal **1996**, 15, 6847–6853.
42. Deardorff, J.A.; Sachs, A.B. Differential effects of aromatic and charged residue substitutions in the RNA binding domains of the yeast poly(A)-binding protein. Journal of Molecular Biology **1997**, 269, 67–81.
43. Eftink, M.R.; Ghiron, C.A. Exposure of tryptophanyl residues in proteins. Quantitative determination by fluorescence quenching studies. Biochemistry **1976**, 15, 672–680.
44. Harada, K.; Martin, S.S.; Frankel, A.D. Selection of RNA-binding peptides in vivo. Nature **1996**, 380, 175–179.
45. Harada, K.; Frankel, A.D. Screening RNA-binding libraries using a bacterial transcription antitermination assay. Methods in Molecular Biology **1999**, 118, 177–187.
46. Barrick, J.E.; Takahashi, T.T.; Balakin, A.; Roberts, R.W. Selection of RNA–binding peptides using mRNA–peptide fusions. Methods **2001**, 23, 287–293.
47. Austin, R.J.; Xia, T.; Ren, J.; Takahashi, T.T.; Roberts, R.W. Designed arginine-rich RNA-binding peptides with picomolar affinity. Journal of the American Chemical Society **2002**, 124, 10966–10967.
48. Van Gilst, M.R.; Rees, W.A.; Das, A.; von Hippel, P.H. Complexes of N antitermination protein of phage lambda with specific and nonspecific RNA target sites on the nascent transcript. Biochemistry **1997**, 36, 1514–1524.
49. Ellington, A.D.; Szostak, J.W. In vitro selection of RNA molecules that bind specific ligands. Nature **1990**, 346, 818–822.
50. Abdelkafi, M.; Leulliot, N.; Baumruk, V.; Bednarova, L.; Turpin, P. Y.; Namane, A.; Gouyette, C.; Huynh-Dinh, T.; Ghomi, M. Structural features of the UCCG and UGCG tetraloops in very short hairpins as evidenced by optical spectroscopy. Biochemistry **1998**, 37, 7878–7884.
51. Leulliot, N.; Baumruk, V.; Abdelkafi, M.; Turpin, P.Y.; Namane, A.; Gouyette, C.; Huynh-Dinh, T.; Ghomi, M. Unusual nucleotide conformations in GNRA and UNCG type tetraloop hairpins: evidence from Raman markers assignments. Nucleic Acids Research **1999**, 27, 1398–1404.
52. Dale, T.; Smith, R.; Serra, M.J. A test of the model to predict unusually stable RNA hairpin loop stability. RNA **2000**, 6, 608–615.

APPENDIX

As seen in Figure A1 (a), the mobility of the NTS RNA at 20°C resembled that of hairpin-loop DNAs with 17 or 18 nts length (HP17 and HP18) but

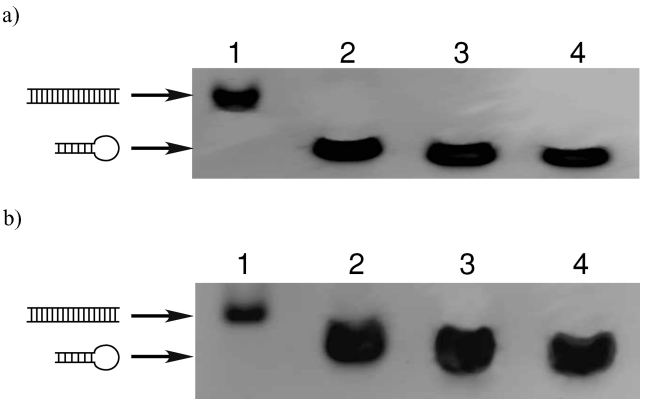

FIGURE A1 20% polyacrylamide gel electrophoresis showing the mobility of 5′–TTTGTATCTCA-ATTTAT–3′/5′–ATAAATTGAGATACAAA–3′ (DX 17), 5′–AGCTGGCGGAAGCCAGCT–3′ (HP 18), 5′–AGCTGGCGGAAGCCAGC–3′ (HP 17), and the NTS RNA from lane 1 (left) to lane 4 (right). Electrophoresis was done (a) for 14 h at 20°C and (b) for 7 h at 50°C, and then the gels were stained by ethidium bromide.

was different from the mobility of a 17 base-paired double-stranded DNA (DX17). Same tendency could be seen in the PAGE experiment at 50°C (b). These results from the PAGE experiments indicated that the NTS RNA fold into hairpin-loop structure at both temperatures, 20 and 50°C.